



Short communication

# A novel one-pot synthesized CuCe-SAPO-34 catalyst with high NH<sub>3</sub>-SCR activity and H<sub>2</sub>O resistance

Can Niu<sup>a,b</sup>, Xiaoyan Shi<sup>a,b,\*</sup>, Kuo Liu<sup>a</sup>, Yan You<sup>a</sup>, Shaoxin Wang<sup>a</sup>, Hong He<sup>a</sup><sup>a</sup> State Key Joint Laboratory of Environment Simulation and Pollution Control, Research Center for Eco-Environment Sciences, Chinese Academy of Sciences, Beijing 100085, China<sup>b</sup> University of Chinese Academy of Sciences, Beijing 100049, China

## ARTICLE INFO

## Article history:

Received 1 February 2016

Received in revised form 1 April 2016

Accepted 11 April 2016

Available online 13 April 2016

## Keywords:

CuCe-SAPO-34

One-pot synthesized hydrothermal method

H<sub>2</sub>O resistanceNH<sub>3</sub>-SCR

## ABSTRACT

CuCe-SAPO-34 catalysts based on the one-pot hydrothermal synthesis method were prepared for the first time. The addition of Ce suppressed the formation of CuO and increased the amount of active Cu<sup>2+</sup>, resulting in better NH<sub>3</sub>-SCR activity than Cu-SAPO-34. Ce greatly improved the H<sub>2</sub>O resistance during the SCR process by stabilizing the zeolite structure and obstructing the transformation of active Cu<sup>2+</sup> into inactive forms.

© 2016 Elsevier B.V. All rights reserved.

## 1. Introduction

Copper-containing small-pore zeolites such as Cu-SAPO-34 and Cu-SSZ-13 have been attracting increasing attention as superior NH<sub>3</sub>-SCR catalysts [1–6]. The Cu-SAPO-34 catalyst showed excellent SCR activity over a wide range of temperature and quite outstanding hydrothermal stability at high temperatures [7–9].

However, it was reported that deactivation of Cu-SAPO-34 can take place in the presence of water at low temperatures. K. Leistner et al. [10] reported that after exposure to H<sub>2</sub>O at 70 °C for 9 h, the NO<sub>x</sub> conversion over Cu-SAPO-34 decreased from 87% to 6% at 200 °C. J. Wang et al. [11] found that hydrothermal treatment at 70 °C could lead to the collapse of the Cu-SAPO-34 structure. Therefore, the presence of H<sub>2</sub>O is detrimental to the Cu-SAPO-34 catalyst, and restricts its potential application. Since H<sub>2</sub>O cannot be avoided during the SCR process due to the presence of a certain amount of water in diesel exhaust, there is an urgent need to improve the water resistance of this catalyst.

Recently, Z. Ma [12] and W. Shan [13] found that ceria exhibited superior redox ability, facilitating the SCR performance. X. Dong et al. [14] showed that incorporating CeO<sub>x</sub> into a Cu-SAPO-34 catalyst by the in-situ wetness impregnation method could improve the SCR activity and suppress the nonselective side reactions. Y. Cao et al. [15,16] reported that CuCe-SAPO-34, which was prepared by wet impregnation of Ce-SAPO-34, showed higher SCR activity, and exhibited better high temperature hydrothermal stability and hydrocarbon resistance than

Cu-SAPO-34. Hence, Ce is a promising candidate for improving the NH<sub>3</sub>-SCR performance of catalysts, especially under severe conditions.

Lately, copper-tetraethylenepentamine (Cu-TEPA) has been designed to fit the CHA structure [4], and used in the one-pot hydrothermal synthesis method to prepare Cu-SAPO-34 directly [5] which showed high SCR activity and hydrothermal stability [17]. The method is easy to perform, with facile control of Cu loading, and might be applicable at industrial scale. Therefore, in this study, we attempted to prepare a novel CuCe-SAPO-34 catalyst with excellent H<sub>2</sub>O resistance by the one-pot hydrothermal synthesis method. The effect of Ce on the structural stability, Cu species distribution, NH<sub>3</sub>-SCR performance and H<sub>2</sub>O resistance of Cu-SAPO-34 was investigated.

## 2. Experimental

### 2.1. Catalyst preparation

CuCe-SAPO-34 catalysts, with x representing the Ce/Al molar ratio in the gel, were prepared by the one-pot hydrothermal synthesis method using Cu-TEPA as the Cu source, cerous nitrate as the Ce source, propylamine (PA) as a co-template, pseudoboehmite as the Al source, 85% phosphoric acid as the P source, and fumed silica as the Si source. The molar composition of the synthesis gel was: 1Al:1P:0.25Si:0.06Cu-TEPA:(0.01/0.04/0.06/0.08)Ce(NO<sub>3</sub>)<sub>3</sub>:1.6PA:40H<sub>2</sub>O. The resulting gel was crystallized for 72 h at 180 °C, and calcined in air at 700 °C for 5 h to remove the organic templates. The Cu-SAPO-34 catalyst was prepared by the above method without Ce addition. The catalysts after SCR reaction with 5% H<sub>2</sub>O were designated as used samples. Table S1

\* Corresponding author.

E-mail address: [xyshi@rcees.ac.cn](mailto:xyshi@rcees.ac.cn) (X. Shi).

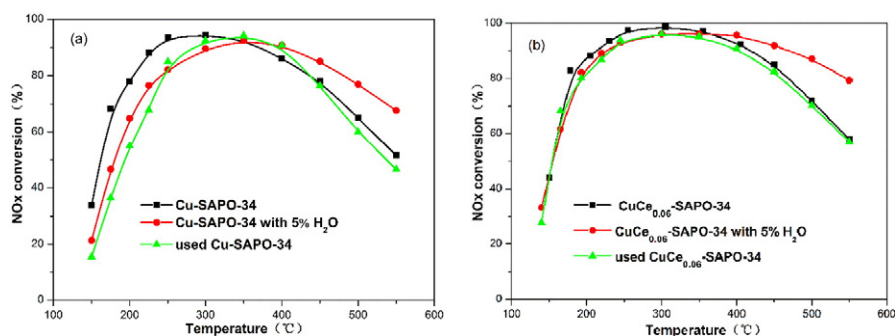


Fig. 1. The NO<sub>x</sub> conversion over (a) Cu-SAPO-34 (b) CuCe<sub>0.06</sub>-SAPO-34 in the absence and presence of H<sub>2</sub>O during the SCR process.

shows that the Cu loading and Si:P:Al molar ratio of all samples were quite close.

## 2.2. Activity measurement

SCR activity tests of the sieved powder catalysts were carried out in a fixed-bed quartz flow reactor at atmospheric pressure. The reaction conditions were as follows: 500 ppm NO, 500 ppm NH<sub>3</sub>, 5 vol.% O<sub>2</sub>, 5% H<sub>2</sub>O (when used), balance N<sub>2</sub> and 500 mL/min total flow rate. During the performance tests, about 60 mg catalyst was used, yielding a rather high GHSV of 400,000 h<sup>-1</sup>. The effluent gas, including NO, NH<sub>3</sub>, NO<sub>2</sub>, and N<sub>2</sub>O, was continuously analyzed by an online NEXUS 670-FTIR spectrometer.

## 2.3. Characterization

The component contents of catalysts were analyzed using an inductively coupled plasma instrument (ICP, OPTMIA 2000DV) with a radial view of the plasma. Powder X-ray diffraction (XRD) measurements were carried out on a computerized PANalytical X'Pert Pro diffractometer with CuKα (λ = 0.15406 nm) radiation. N<sub>2</sub> adsorption/desorption isotherms were measured at -196 °C using a Quantachrome Quadrasorb SI-MP. Prior to the N<sub>2</sub> physical adsorption, the samples were degassed at 300 °C for 5 h. Micropore surface areas and micropore volumes were determined by the t-plot method. The surface morphology of the samples was studied using a Field-Emission Scanning Electron Microscope (FE-SEM, SU-8020). Temperature-programmed reduction with hydrogen (H<sub>2</sub>-TPR) experiment was carried out on a Micromeritics AutoChem 2920 chemisorption analyzer. X-ray photoelectron spectroscopy (XPS) with Al Kα radiation (1486.7 eV) was

used to analyze the oxidation state of copper species on the catalysts' surface (Axis Ultra, Kratos Analytical Ltd).

## 3. Results and discussion

### 3.1. Catalytic activity

As shown in Fig. S1(a), the NO<sub>x</sub> conversion of CuCe<sub>x</sub>-SAPO-34 increased with increasing Ce loading when the Ce/Al molar ratio was less than 0.06 and then decreased for higher Ce loading. The CuCe<sub>0.06</sub>-SAPO-34 showed the best SCR activity among the prepared CuCe<sub>x</sub>-SAPO-34 samples. Hence, we chose CuCe<sub>0.06</sub>-SAPO-34 to compare with Cu-SAPO-34. As shown in Fig. 1(a), the presence of 5% H<sub>2</sub>O decreased the NO<sub>x</sub> conversion of Cu-SAPO-34 below 350 °C, and increased the NO<sub>x</sub> conversion above 350 °C which was speculated that H<sub>2</sub>O could inhibit NH<sub>3</sub> oxidation and side-products during the NH<sub>3</sub> oxidation process at high temperatures [18]. The activity of a used Cu-SAPO-34 sample was tested in dry flue gas. The results showed that the effect of H<sub>2</sub>O on Cu-SAPO-34 was irreversible. As shown in Fig. 1(b), there was negligible influence of H<sub>2</sub>O on the SCR activity of CuCe<sub>0.06</sub>-SAPO-34 below 350 °C, and the NO<sub>x</sub> conversion of this sample increased above 350 °C. As with Cu-SAPO-34, the activity of used CuCe<sub>0.06</sub>-SAPO-34 was retested in dry flue gas. Only a slight loss of SCR activity was observed for the used CuCe<sub>0.06</sub>-SAPO-34 sample. To examine the low temperature hydrothermal stability of Cu-SAPO-34 and CuCe<sub>0.06</sub>-SAPO-34, these two catalysts were treated at 70 °C and 150 °C in 10% H<sub>2</sub>O/air for 12 h. As shown in Fig. S2, CuCe<sub>0.06</sub>-SAPO-34 showed higher stability than Cu-SAPO-34 after the low-temperature hydrothermal aging. This indicated that the addition of Ce into Cu-SAPO-34 might improve the stability of the sample in moist conditions. Furthermore, the high temperature hydrothermal stability of Cu-SAPO-34 and CuCe<sub>0.06</sub>-SAPO-34 were compared as shown in Fig.S1(b), indicating that introducing 0.10 wt.% Ce into Cu-SAPO-34 by the one-pot hydrothermal synthesis method could not significantly affect the hydrothermal stability of Cu-SAPO-34.

### 3.2. XRD

Fig. 2 shows the XRD patterns of fresh and used Cu-SAPO-34 and CuCe<sub>0.06</sub>-SAPO-34 samples. The addition of Ce did not affect the framework or crystallinity of fresh Cu-SAPO-34 as shown in Fig. S3(a). For used Cu-SAPO-34, the intensity of all diffraction peaks decreased significantly. The XRD patterns showed that the crystalline structure was changed by the action of H<sub>2</sub>O [11,19]. However, there was no evident decline of crystallinity for the used CuCe<sub>0.06</sub>-SAPO-34 sample compared to the fresh one. This indicated that Ce ions may replace the proton of the Si—O(H)—Al bond to decrease the concentration of Si—O(H)—Al bonds, preventing the hydrolysis reactions at the acid sites [11,20]. The interaction of H<sub>2</sub>O with other framework atoms appeared to be much weaker and was reversible, improving the stability of the zeolite

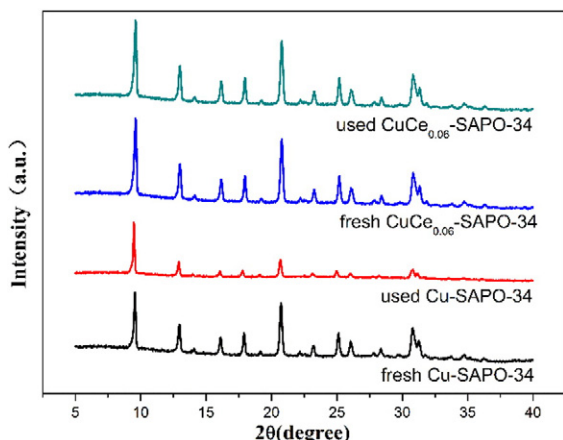


Fig. 2. The XRD results of the fresh and used Cu-SAPO-34 and CuCe<sub>0.06</sub>-SAPO-34.

**Table 1**  
Micropore surface area, micropore volume, Cu species distribution and H<sub>2</sub>/Cu (mol/mol) ratio of the fresh and used Cu-SAPO-34 and CuCe<sub>0.06</sub>-SAPO-34 samples.

Samples	Micropore surface area, m <sup>2</sup> /g	Micropore volume, cm <sup>3</sup> /g	Proportion of total copper species, %			H <sub>2</sub> /Cu, mol/mol
			Cu <sup>2+</sup>	CuO	Cu <sup>+</sup>	
Fresh Cu-SAPO-34	533.6	0.28	52	23	25	0.62
Used Cu-SAPO-34	480.2	0.24	35	61	4	0.81
Fresh CuCe <sub>0.06</sub> -SAPO-34	519.7	0.28	64	3	33	0.52
Used CuCe <sub>0.06</sub> -SAPO-34	513.6	0.28	69	3	28	0.52

[19]. The higher stability of the CHA structure in CuCe<sub>0.06</sub>-SAPO-34 contributed to its higher water resistance in comparison with Cu-SAPO-34.

### 3.3. N<sub>2</sub> adsorption/desorption

According to the N<sub>2</sub> adsorption/desorption results as shown in Table 1, the micropore surface area of Cu-SAPO-34 and CuCe<sub>0.06</sub>-SAPO-34 were 533.6 and 519.7 m<sup>2</sup>/g respectively, and the micropore volume of those two samples were same. It indicated that the addition of Ce did not result in the significantly decrease of the micropore surface area and micropore volume of Cu-SAPO-34. Therefore, the possibility of blockage Ce due to its large kinetic diameter can be ignored. Furthermore, the used CuCe<sub>0.06</sub>-SAPO-34 contained almost all of the micropore surface area and micropore volume, revealing that the addition of Ce can stabilize the framework structure in consistent with the results of XRD and SEM (Fig. S4).

### 3.4. H<sub>2</sub>-TPR

H<sub>2</sub>-TPR was used to identify and quantify the copper species distribution in the catalysts, and the results are shown in Fig. 3. The ratio of Cu species to total copper species were calculated from the results of H<sub>2</sub>-TPR, and shown in Table 1. It showed that the ratio of Cu<sup>2+</sup> to total

copper loadings increased from 52 to 64% for the fresh CuCe<sub>0.06</sub>-SAPO-34 and Cu-SAPO-34 sample. This suggested that the addition of Ce to Cu-SAPO-34 could increase the amount of isolated Cu<sup>2+</sup> ions which are active sites for SCR reaction at low temperatures [21,22], resulting in the observed increase of SCR activity below 350 °C. Similar results were reported by Y. Cao et al. [15], that the interaction between cerium and copper could improve the dispersion of copper species and increase the amount of isolated Cu<sup>2+</sup> ions. Meanwhile, the addition of Ce decreased the amount of CuO, which could lead to non-selective oxidation of NH<sub>3</sub> at high temperatures [23,24]. CuCe<sub>0.06</sub>-SAPO-34 showed lower NH<sub>3</sub> oxidation at high temperatures (Fig. S5), leading to better SCR activity than Cu-SAPO-34 above 350 °C.

The ratio of Cu<sup>2+</sup>/Cu loading was 0.64 for fresh and 0.69 for used CuCe<sub>0.06</sub>-SAPO-34, however, in the case of Cu-SAPO-34, the Cu<sup>2+</sup>/Cu loading decreased from 0.52 to 0.35, with obviously CuO formation. The Cu loadings of Cu-SAPO-34 (3.29%) and CuCe-SAPO-34 (3.28%) was quite same (Table S1). The data indicated that the migration of copper species and formation of CuO occurred for the used Cu-SAPO-34 sample, in accordance with a previous report [10], resulting in the deactivation of Cu-SAPO-34 after the SCR reaction with H<sub>2</sub>O and the failure of the catalyst's ability to recover SCR activity in the absence of H<sub>2</sub>O (Fig. 1a). In contrast, little change in the copper species distribution was observed on the used CuCe<sub>0.06</sub>-SAPO-34 sample. This result further

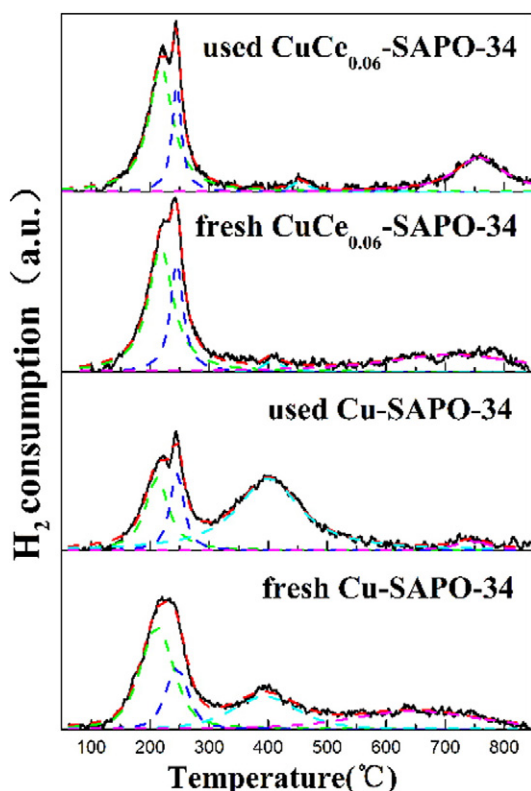


Fig. 3. The H<sub>2</sub>-TPR results of the fresh and used Cu-SAPO-34 and CuCe<sub>0.06</sub>-SAPO-34.

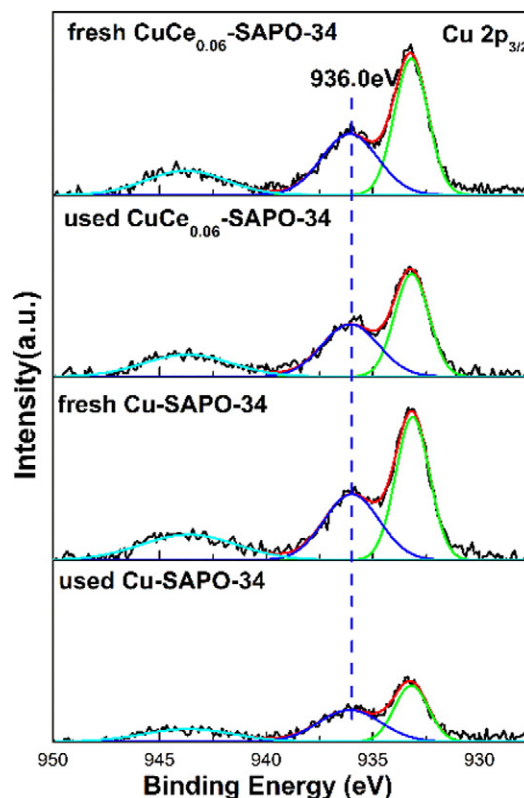


Fig. 4. Cu 2p<sub>3/2</sub> XPS spectra of fresh and used Cu-SAPO-34 and CuCe<sub>0.06</sub>-SAPO-34.

confirmed the higher stability of  $\text{Cu}^{2+}$  ions on  $\text{CuCe}_{0.06}\text{-SAPO-34}$  than on  $\text{Cu-SAPO-34}$ , leading to the excellent water resistance of the  $\text{CuCe}_{0.06}\text{-SAPO-34}$  catalyst during the SCR reaction (Fig. 1b).

### 3.5. XPS

The XPS results of the fresh and used  $\text{Cu-SAPO-34}$  and  $\text{CuCe}_{0.06}\text{-SAPO-34}$  samples are shown in Fig. 4.  $\text{Cu } 2p_{3/2}$  peaks were observed in the ranges of 930.0–940.0 eV. The  $\text{Cu } 2p_{3/2}$  peak around 936.0 eV as well as the satellite peak around 940.0–948.0 eV is used as a characteristic to determine  $\text{Cu}^{2+}$  [25,26]. The peaks of  $\text{Cu } 2p_{3/2}$  are further discussed in the terms of the effect of water on Cu valence state on the surface of the catalysts. It was found that the relative concentration of isolated  $\text{Cu}^{2+}$  on the surface of used  $\text{Cu-SAPO-34}$  decreased significantly after SCR process involved with water which may be associated with the agglomeration of  $\text{CuO}$  [26]. Less  $\text{Cu}^{2+}$  on the surface of used  $\text{Cu-SAPO-34}$  sample led to the performance decline for  $\text{NO}_x$  removal in a certain degree. However, the change of isolated  $\text{Cu}^{2+}$  concentration on used  $\text{CuCe}_{0.06}\text{-SAPO-34}$  was not very obvious, indicating that the copper species was not affected by water evidently in accordance with the  $\text{H}_2\text{-TPR}$  results.

### 4. Conclusions

The effects of  $\text{H}_2\text{O}$  during the SCR process on  $\text{Cu-SAPO-34}$  and  $\text{CuCe}_{0.06}\text{-SAPO-34}$  catalysts were investigated by ICP, BET, SEM, XRD,  $\text{H}_2\text{-TPR}$  and XPS. The results indicated that the introduction of Ce could improve the  $\text{NH}_3\text{-SCR}$  performance and  $\text{H}_2\text{O}$  resistance of  $\text{Cu-SAPO-34}$ . Modification by Ce could decrease the amount of  $\text{CuO}$  and increase  $\text{Cu}^{2+}$  ions in  $\text{Cu-SAPO-34}$ . The addition of Ce could stabilize the framework structure and active  $\text{Cu}^{2+}$  ions in the presence of  $\text{H}_2\text{O}$  during the SCR process.

### Acknowledgments

This work was financially supported by the National Natural Science Foundation of China (51578536, 51278486, 21303247).

### Appendix A. Supplementary data

Supplementary data to this article can be found online at <http://dx.doi.org/10.1016/j.catcom.2016.04.007>.

### References

- [1] J.H. Kwak, R.G. Tonkyn, D.H. Kim, J. Szanyi, C.H.F. Peden, *J. Catal.* 275 (2010) 187–190.
- [2] D.W. Fickel, E. D'Addio, J.A. Lauterbach, R.F. Lobo, *Appl. Catal., B* 102 (2011) 441–448.
- [3] S.T. Korhonen, D.W. Fickel, R.F. Lobo, B.M. Weckhuysen, A.M. Beale, *Chem. Commun. (Camb.)* 47 (2011) 800–802.
- [4] L. Ren, L. Zhu, C. Yang, Y. Chen, Q. Sun, H. Zhang, C. Li, F. Nawaz, X. Meng, F.S. Xiao, *Chem. Commun. (Camb.)* 47 (2011) 9789–9791.
- [5] M.-F. Raquel, M. Moliner, C. Franch, A. Kustov, A. Corma, *Appl. Catal., B* 127 (2012) 273–280.
- [6] X. Liu, X. Wu, D. Weng, Z. Si, *Catal. Commun.* 59 (2015) 35–39.
- [7] L. Ma, Y. Cheng, G. Cavataio, R.W. McCabe, L. Fu, J. Li, *Chem. Eng. J.* 225 (2013) 323–330.
- [8] Q. Ye, L. Wang, R.T. Yang, *Appl. Catal. A Gen.* 427 (2012) 24–34.
- [9] D. Wang, J. Yasser, Y. Liu, M.K. Sharma, J. Luo, J. Li, K. Kamasamudram, W.S. Epling, *Appl. Catal., B* 165 (2015) 438–445.
- [10] K. Leistner, L. Olsson, *Appl. Catal., B* 165 (2015) 192–199.
- [11] J. Wang, D. Fan, T. Yu, J. Wang, T. Hao, X. Hu, M. Shen, W. Li, *J. Catal.* 322 (2015) 84–90.
- [12] Z. Ma, D. Weng, X. Wu, Z. Si, B. Wang, *Catal. Commun.* 27 (2012) 97–100.
- [13] W. Shan, F. Liu, Y. Yu, H. He, C. Deng, X. Zi, *Catal. Commun.* 59 (2015) 226–228.
- [14] X. Dong, J. Wang, H. Zhao, Y. Li, *Catal. Today* 258 (2015) 28–34.
- [15] Y. Cao, S. Zou, L. Lan, Z. Yang, H. Xu, T. Lin, M. Gong, Y. Chen, *J. Mol. Catal. A Chem.* 398 (2015) 304–311.
- [16] Y. Cao, L. Lan, X. Feng, Z. Yang, S. Zou, H. Xu, Z. Li, M. Gong, Y. Chen, *Catal. Sci. Technol.* 5 (2015) 4511–4521.
- [17] M.-F. Raquel, M. Moliner, P. Concepcion, J.R. Thogersen, A. Corma, *J. Catal.* 314 (2014) 73–82.
- [18] T. Yu, J. Wang, M. Shen, J. Wang, W. Li, *Chem. Eng. J.* 264 (2015) 845–855.
- [19] F.D.P. Mees, L.R.M. Martens, M.J.G. Janssen, A.A. Verberckmoes, E.F. Vansant, *Chem. Commun.* (2003) 44–45.
- [20] F. Gao, E.D. Walter, N.M. Washton, J. Szanyi, C.H.F. Peden, *ACS Catal.* 3 (2013) 2083–2093.
- [21] J. Xue, X. Wang, G. Qi, J. Wang, M. Shen, W. Li, *J. Catal.* 297 (2013) 56–64.
- [22] L. Xie, F. Liu, L. Ren, X. Shi, F.S. Xiao, H. He, *Environ. Sci. Technol.* 48 (2014) 566–572.
- [23] D. Wang, L. Zhang, J. Li, K. Kamasamudram, W.S. Epling, *Catal. Today* 231 (2014) 64–74.
- [24] L. Wang, W. Li, G. Qi, D. Weng, *J. Catal.* 289 (2012) 21–29.
- [25] L. Pang, C. Fan, L. Shao, K. Song, J. Yi, X. Cai, J. Wang, M. Kang, T. Li, *Chem. Eng. J.* 253 (2014) 394–401.
- [26] J. Wang, Z. Peng, Y. Chen, W. Bao, L. Chang, G. Feng, *Chem. Eng. J.* 263 (2015) 9–19.